

PATENT

IN THE UNITED STATES PATENT AND TRADEMARK OFFICE

In re application of: Michel Sayag

Attorney Docket No.: SAY1P004D1

Application No. 10/789,547

Examiner: Shun K. Lee

Filed: February 26, 2004

Group: 2878

Title: LIGHT STIMULATING AND
COLLECTING METHODS AND APPARATUS
FOR STORAGE-PHOSPHOR IMAGE PLATES

DECLARATION UNDER 37 C.F.R. 1.132

I, Michel Sayag, declare the following:

1. I am the inventor of the invention set forth in the above referenced application.
2. I have a significant and sophisticated expertise relating to charge-coupled devices (CCDs) and x-ray image sensors. I have an extensive and successful technical and marketing background, which encompasses more than fifteen years of product and business development experience at Lockheed Martin Fairchild. I am an inventor on ten key patents in the field of electronic imaging. As Lockheed Martin Fairchild's Director of International Marketing from 1991 to 2000, I developed a number of medical and dental imaging products. I earned a Bachelor in Physics from Saint-Louis College in Paris, France, and a Masters degree in Electro-Optical Engineering from the Institute of Optics in Orsay, France. I am a member of the International Society for Optical Engineering (SPIE).

3. Clarification about the differences between Mueller's "x-ray cassette" and a film-like cassette (cassette similar in size to a standard radiographic film cassette)

In US patent 6,373,074, Mueller never teaches how to incorporate a reading apparatus in an enclosure similar in size to a standard radiographic film cassette. Mueller mentions an "x-ray cassette", which is in fact a misnomer for an enclosure containing a digital x-ray sensor (the "cassette" doesn't generate any x-rays but rather houses an x-ray image sensor). Mueller never describes an enclosure similar in size to a standard radiographic film cassette (i.e., able to fit in the cassette tray of an x-ray unit) but rather an enclosure which can be "integrated directly in an x-ray unit" (column 3, line 66). Further on, Mueller discusses the possibility for his enclosure to be "inserted directly into a x-ray table" (column 10, line 47).

The only dimension Mueller mentions is a 45mm enclosure thickness, which does not match any known radiographic film cassette but does correspond to the thickness of most cassette holders, commonly referred to in the medical industry as "buckys." Mueller clearly describes an enclosure which can be integrated directly in an x-ray unit, signifying an enclosure

which can be inserted in the x-ray table, not in the cassette tray of the table's bucky. Because of its size, Mueller's enclosure can fit in the x-ray table as a replacement for the bucky but clearly cannot fit in the cassette tray.

When Mueller writes (column 10, line 52): "the x-ray cassette can be manufactured with very small dimensions", he is comparing it to the reading devices currently sold by Mueller's assignee which are the size of household refrigerators. Mueller's enclosure is referred to in the industry as a "digital bucky." There are already a number of such digital buckys on the market (CSDI-22 from Canon Medical, StingRay from InfiMed, QuixDB from Edge Medical and Clarity from Cares Built). Mueller's assignee (Agfa) has announced a digital bucky based on Mueller's design (see Fig. 12 from the Agfa publication provided with the last response) but it is not yet available. At first glance digital buckys seem to be very similar to the digital radiography cassette made possible by the present invention, because they both claim to be compatible with existing x-ray generators and tables. They are not.

Digital buckys can replace existing film buckys but the process is usually irreversible. Because of their size, weight and fragility, digital buckys are permanently installed and cannot be moved around. As a result, the equipment can no longer accommodate film cassettes; if the digital bucky fails, the x-ray equipment becomes unusable. This also implies that two separate sensors are needed to equip a typical x-ray room, which often consists of an x-ray table and a wall-mount stand. In addition, digital buckys cannot be used for mobile or portable x-ray applications (i.e., bedside exams). And, since the film bucky must be removed in order to install a digital bucky, the x-ray equipment must be modified and its electrical and mechanical interfaces changed. This leads to serious FDA re-certification issues as well as warranty and service coverage issues. Any automatic positive beam limitation (PBL) capability in the x-ray equipment must be disabled and the collimation of the x-ray beam must be manually adjusted instead of being automatically adjusted by the film bucky. None of these limitations exist with the digital radiography cassette of the present invention since it is similar in size to a standard radiographic film cassette and can therefore be inserted in the cassette tray (i.e., into the bucky) without any modifications to the x-ray table.

4. Clarification about the need for optics in Mueller's reproduction device

Mueller calls the imaging system between the phosphor plate and the CCD line the reproduction device (column 5, line 10). It is important to remember that, unlike a flying-spot scanner which stimulates the plate one point at a time, Mueller's apparatus stimulates the plate one line at a time and therefore requires a reproduction device to image the stimulated line onto the CCD line array. Without such reproduction device, nothing would prevent light generated at one location along the stimulated area of the plate to reach many pixels on the CCD line array. Similarly, nothing would prevent light generated at different locations of the plate to reach the same pixel of the CCD line array. *Thus, without a reproduction device (e.g., a Selfoc lens or its equivalent) capable of forming an image of the plate onto the CCD line array, the CCD line array is unable to perform its task and Mueller's reading apparatus cannot function.* Contrary to the Examiner's assertion, Mueller neither suggests that the reproduction device is unnecessary nor that his apparatus would work without it.

There is sometimes some confusion about the need for a reproduction device because unlike a line-by-line reading apparatus, a conventional point-by-point reading apparatus (i.e., flying-spot scanner) does not require a reproduction device. In a flyer-spot scanner, the reading

of the plate is achieved by stimulating the plate one point at a time and thus the detector has only one pixel (generally a photomultiplier). With such an approach, no imaging optics is necessary to collect the stimulated light since it can only come from one point at a time. On the other hand, *scanning* optics are still necessary to focus the laser spot onto the plate. The size of the laser spot on the plate is determined by the scanning optics and greatly affects the resolution of the apparatus.

To the undersigned's knowledge, there are only two methods to implement a reproduction device in a line-by-line reading apparatus: contact imaging or aerial imaging.

Contact imaging is by far the most compact way to image the plate onto the CCD line array. In such an approach, the plate is placed in contact with the CCD line array. Light emitted at a given location on the plate is directly captured by the CCD pixels adjacent to it and cannot propagate further. With contact imaging, it is possible to manufacture a CCD assembly (which Mueller calls a "receiving device") which can be incorporated in an enclosure similar in size to a standard radiographic film cassette (i.e., 0.6 inches thick). As clearly shown in Figs. 22 and 24 of the present application, the receiving device must be much less than 0.6 inches in order to fit in an enclosure for which the outside dimension is 0.6 inches.

By relying on contact imaging, the present invention teaches how a very short optical path length can be achieved (e.g., as shown in fig. 10B). Other benefits of contact imaging are that no focusing mechanism is required and that maximum light collection may be achieved (equivalent to a numerical aperture of 1).

The reason the present invention can use contact imaging is that the section of the plate imaged onto the CCD line array is stimulated from inside the plate (light diffusing laterally) rather than from outside the plate. Mueller cannot use contact imaging because he only teaches how to stimulate the plate from the outside. *If Mueller's "receiving device," e.g., the CCD line, was to be placed in contact with the plate, it would block the stimulating light from reaching the plate.* Mueller must therefore use aerial imaging.

Mueller describes two conventional types of aerial imaging optics, one based on Selfoc arrays (many Selfoc lenses bundled together) and one based on a microlens arrays. Selfoc arrays are commonly used in facsimile machines and form an image with a 1:1 magnification. Selfoc arrays are composed of one or more rows of gradient index lenses. The images from adjacent lenses overlap and form a continuous erect image. The index gradient inside each lens determines the resolution of the Selfoc array and it should be noted that, unlike conventional fiber optic faceplates, Selfoc arrays can image features smaller than the size of each lens. Mueller recognizes this fact and mentions that "[a] Selfoc lens can be provided for each stimuable point of the line of the phosphor plate 15, however, this is not required for the invention" (column 5, lines 12-14).

That is, Mueller states that is not necessary to have a Selfoc lens for each point of the line, meaning the Selfoc array does not have to contain as many lenses as the number of photodetectors (column 5, lines 5-6). This does not, however, mean that no intervening optical system is needed. Rather, as discussed above, some mechanism is required to prevent light intended for one pixel from impinging on adjacent pixels. *Without such a mechanism, Mueller would be inoperative.* In fact, Mueller suggests that a microlens array can be used as an alternative to the Selfoc array (column 5, lines 26-27).

A plausible reason Mueller never teaches how to incorporate the reading apparatus in an enclosure similar in size to a standard radiographic film cassette, is that his reproduction device (which relies on aerial imaging) cannot be fit into an enclosure having such a thickness, i.e., 0.6 inches. Aerial imaging requires a minimum optical path length significantly greater than 0.6 inches in order to provide the necessary image quality with an acceptable numerical aperture. High numerical aperture is necessary to collect as much light as possible (if not, more x-ray dose is necessary to produce a diagnostic-quality image). However, high numerical aperture also implies very low depth of focus, implying a complex mechanical fixture to adjust focus across the entire CCD line array.

The differences between contact imaging and aerial imaging may be further understood with reference to the materials provided by the undersigned in connection with the previous office action response.

5. I hereby declare that all statements made herein of my own knowledge are true and that all statements made on information and belief are believed to be true. I further declare that these statements are made with the knowledge that willful false statements and the like so made are punishable by fine or imprisonment, or both (under Section 1001 of Title 18 of the United States Code), and that such willful false statements may jeopardize the validity of the application or any patent issued thereon.

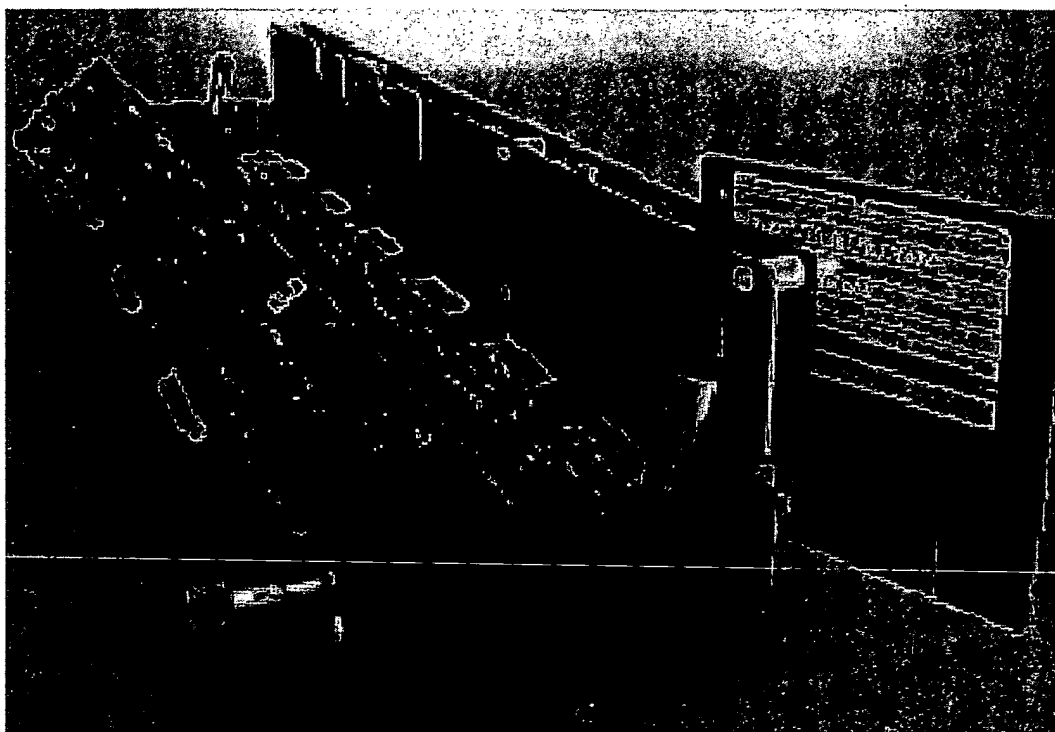
Date

April 20, 2005

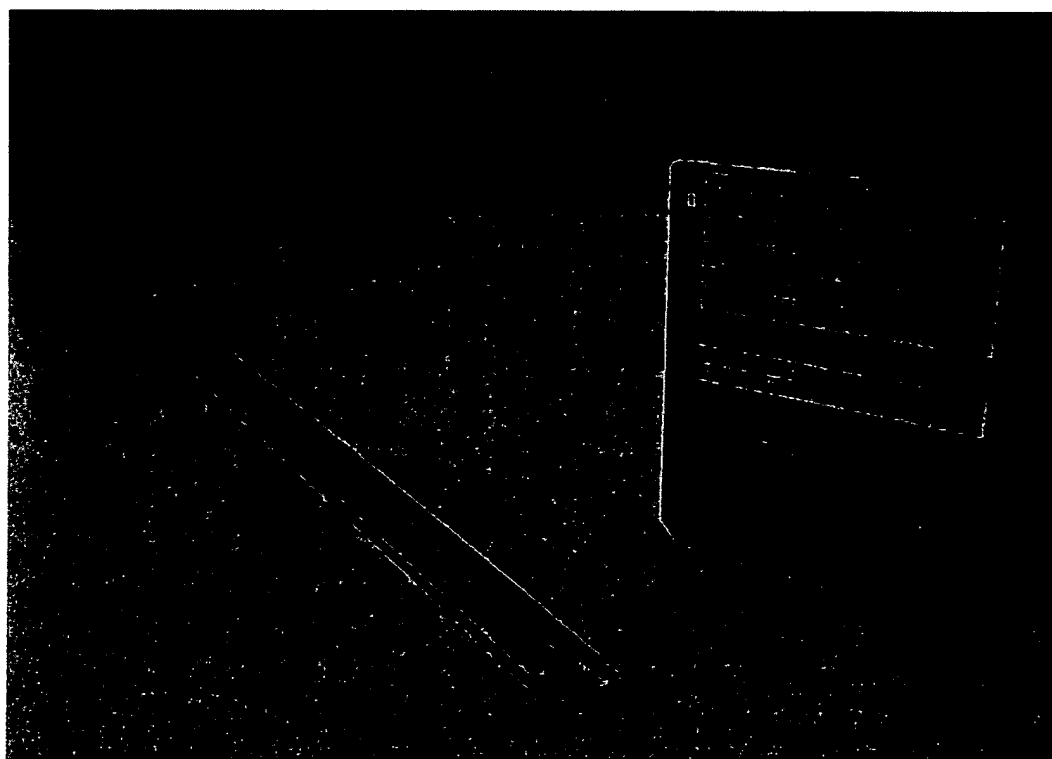
Michel Sayag:

ds sayag

Size difference between Muller and Sayag designs



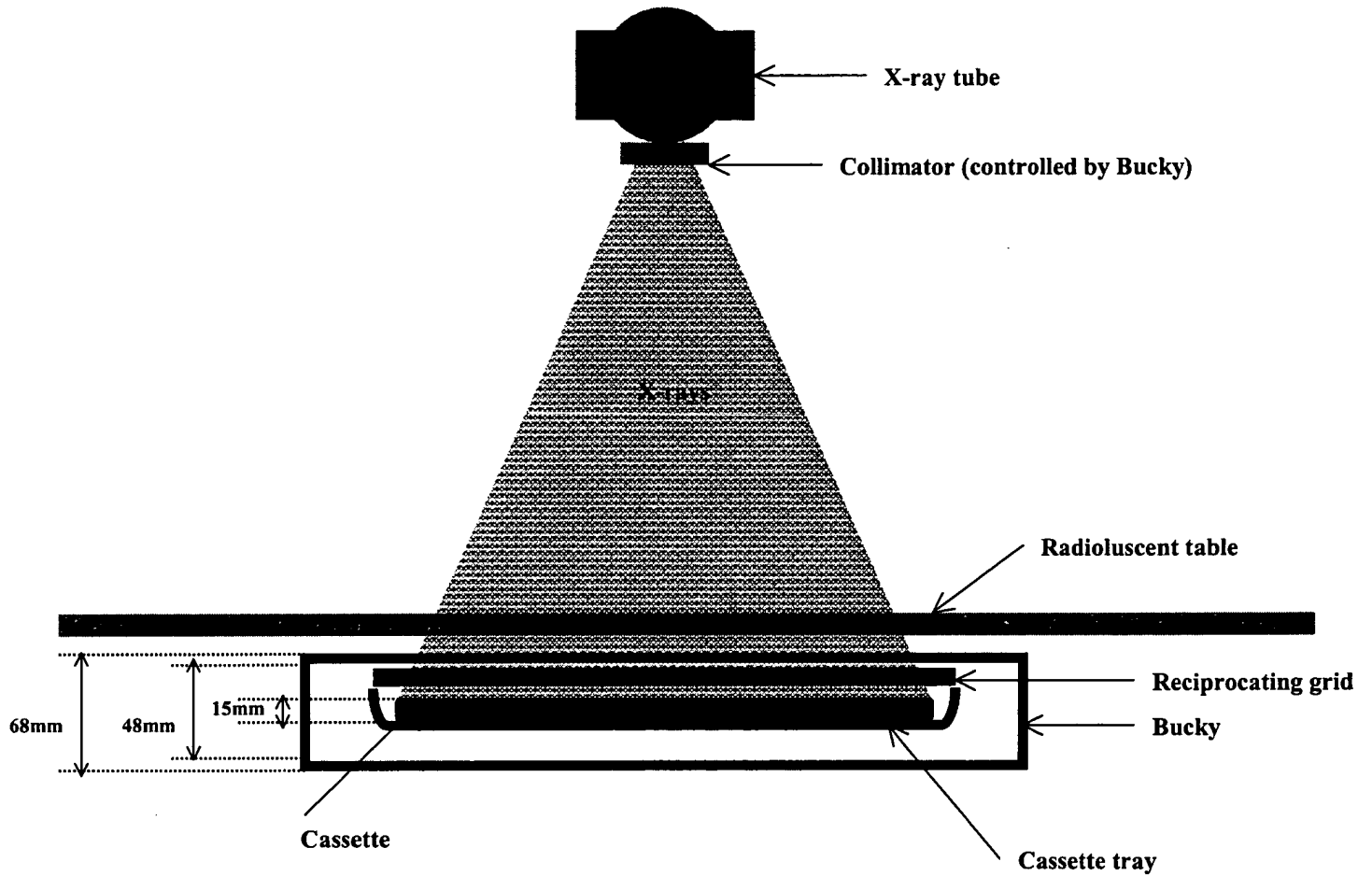
Muller design (per Agfa publication)



Sayag design

BEST AVAILABLE COPY

X-ray Machine Components



Bucky dimensions per Poersch drawing (http://www.poerschmetal.com/Bucky_folder/Bucky.html)

BEST AVAILABLE COPY

Digital Bucky versus Digital X-ray Cassette

Muller enclosure (Bucky) insertable in existing x-ray units

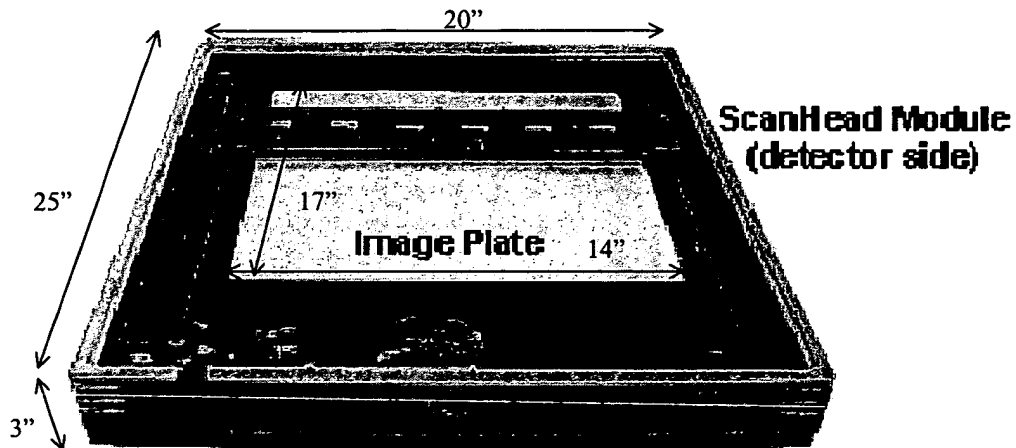
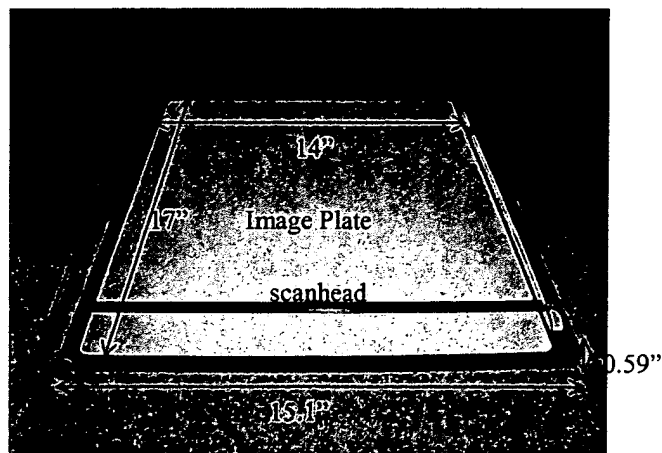


Figure 12. View inside a CR flat panel containing the ScanHead[®] module. The stimulation section is underneath the image plate.

Agfa's original text relating to Fig.12:

"Fig. 12 shows a prototype of a ScanHead[®]-based flat-panel CR system that might be used for portable radiography or as the capture module inside a Bucky table."

Sayag enclosure (cassette) insertable in cassette tray of existing x-ray units



Dimensions taken from Sayag's Fig. 23 (no new information added)

New high-speed scanning technique for Computed Radiography

Ralph Schaetzing¹, Robert Fasbender, Peter Kersten
Agfa-Gevaert AG., HealthCare, Munich, Germany

ABSTRACT

The natural luminescence decay time of storage phosphors limits the scan speed of today's flying-spot Computed Radiography (CR) scanners, since this "afterglow" emission degrades the MTF along the fast-scan direction. Although this sharpness loss can be compensated to some extent with image processing, there is a decrease of signal-to-noise in the process. Higher scan speeds can also decrease the total amount of signal captured at each point, that is, the read-out depth. One may reduce these problems by scanning entire lines at once, rather than points. However, this can create other problems related to stimulation and collection efficiency, system gain, sharpness, and noise. We have developed a new scanning engine containing a linear, laser-diode-based stimulation source and a light collection/detection system with specially designed optics and multiple, linear, asymmetric CCDs. The stimulation/collection systems are housed in a compact, movable read-head that scans quickly (43x43 cm in 5 s, independent of resolution) over a stationary image plate (IP). We evaluated this so-called ScanHead[®] system with conventional powder IPs and with new CsBr:Eu²⁺ needle-based IPs. We also compared it to a conventional flying-spot scanner. Image quality results differed depending on plate type. DQE values for conventional powder IPs in the prototype scanner were comparable to today's state-of-the-art commercial CR systems (DQE(0)~0.25-0.28). DQE values for prototype needle IPs were significantly better than for powder IPs (DQE(0) ~0.58-0.60) and comparable to those quoted for flat-panel DR systems based on CsI:TI.

Keywords: Computed Radiography, CR, storage phosphor, digital radiography, DR, image quality, scanning, needle image plate, IP, CsBr

1. INTRODUCTION

Although some of the technologies needed to do Computed Radiography (CR) have existed for over 60 years¹, the first commercial CR system was introduced only about 20 years ago². Today, CR is a clinically accepted imaging modality for practically every exam type, and many manufacturers have entered the market with CR systems and related equipment. Over the last 20 years, manufacturers have been able to decrease the physical size and increase the throughput of CR systems considerably, while increasing their image quality. However, there are some inherent limitations to these tendencies.

All commercial CR scanners today use, more or less, the principle of flying-spot scanning, in which a tightly focused laser beam is used to stimulate the latent image in a moving storage phosphor screen (image plate) one point at a time over the entire screen surface (Fig. 1). Through appropriate collection optics, some (preferably large) fraction of the emitted light from each point is captured, converted by a photodetector (usually a photomultiplier tube) into an analog electrical signal, then sampled and quantized to produce a digital image. The hardware needed to produce and deflect the laser beam, as well as the components needed to collect the emitted light and convert it into an electrical signal require a certain amount of space, which makes it difficult to reduce indefinitely the physical size of flying-spot scanners. In addition, these discrete components add cost and complexity.

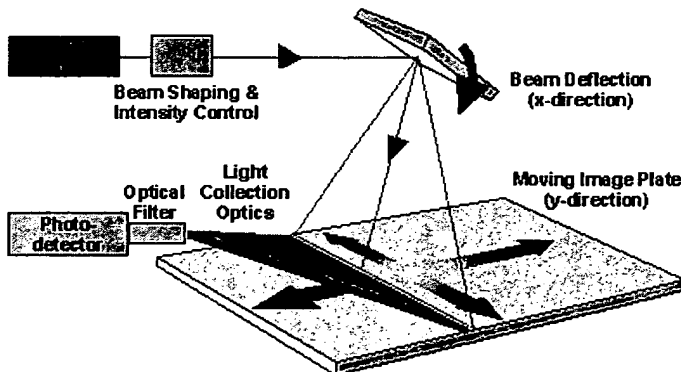


Figure 1. Schematic diagram of the components in a flying-spot scanner.

¹ ralph.schaetzing.rs@germany.agfa.com; Phone: +49(89)6207-3352; FAX: +49(89)6207-7619;
<http://www.agfa.com/healthcare>; Agfa-Gevaert AG, Tegernseer Landstr. 161, 81539 Munich, Germany

The throughput of a flying-spot CR scanner depends on many factors¹, one of them being how much of the stored latent image in the IP the scanner must/can extract in order to make an output image with reasonable image quality (this signal, a component of *system gain*, largely determines SNR). The fraction of stored signal released from the IP during scanning, called the *read-out depth*, depends on the amount of stimulation energy deposited per unit screen area, which is proportional to the incident laser intensity and exposure time. This is illustrated in Fig. 2³. Increasing the exposure increases the total emitted signal until the stored latent image is essentially depleted (any remaining signal must be erased before the IP can be reused). The read-out depth per pixel depends on the amount of time the laser beam spends "over" the pixel area, also known as the *dwell time*. Dwell time is inversely proportional to beam velocity (see Fig. 3).

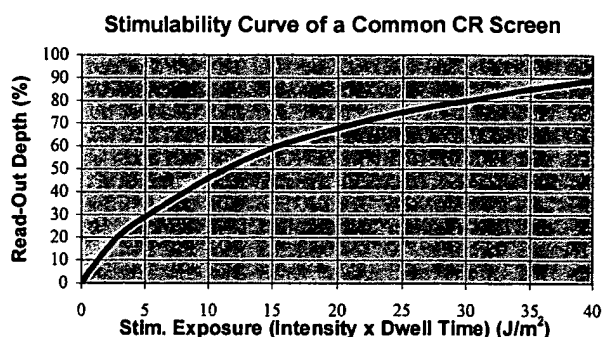


Figure 2. Stimulability curve for a common storage phosphor screen³. The fraction of stored signal read out increases with stimulating exposure until the latent image has been essentially depleted (any remaining signal on the IP must be erased before the next use).

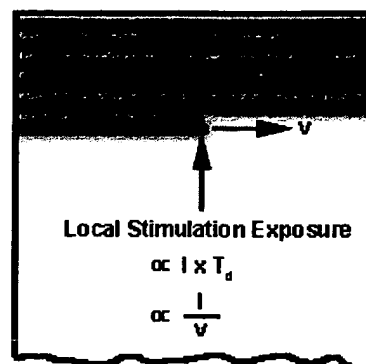


Figure 3. Schematic diagram of an IP being scanned in a flying-spot scanner. The local exposure is proportional to the intensity, I , and the dwell time, T_d , of the laser in that area. T_d is inversely proportional to the beam velocity, v .

So, the fundamental throughput trade-off in a flying-spot scanner is scan time vs. signal. Higher scan speeds reduce scan time and, therefore, increase throughput, all other things remaining constant. However, higher scan speeds also reduce dwell time, which lowers read-out depth and decreases image quality. From Fig. 3, one can see that increasing the laser intensity can compensate for this exposure reduction at higher velocities. However, increasing the laser intensity also broadens the incident beam within the phosphor layer (due to light scattering) which reduces MTF and produces a loss of image quality.

An additional throughput trade-off with flying spot scanners is "afterglow." If the stimulating laser beam exposing a storage phosphor screen were turned off suddenly, the screen would continue to emit light for a short, material-dependent period of time, called the *luminescence decay time*, τ . The luminescence decay times of a few common storage phosphor materials, $\text{BaFBr}_{1-x}\text{Eu}^{2+}$ being the most commonly used today, are listed in Table 1^{4, 5, 6}. If the dwell time gets short enough that it begins to approach this natural decay time, the light being collected at the current beam position contains "leftover" light still coming from the previous beam position(s). As a result, the image signal is effectively smeared in the fast-scan direction, lowering the MTF in that direction. This puts an upper limit on the throughput of flying-spot scanners (modern CR flying-spot scanners have dwell times on the order of 1-6 μs , i.e., about $1.5-8\tau$ for a BaFBr screen). Since the signal decay/blur characteristics are usually known, one may use image restoration techniques⁷ effectively to undo this smearing effect, but only at the expense of lower SNR in the final image.

Storage Phosphor	Luminescence Decay Time, τ
SrS:Ce,Sm	~25 ns
RbBr:Tl	350 ns
CsBr:Eu^{2+}	700 ns
$\text{BaFBr}_{1-x}\text{Eu}^{2+}$	~750 ns

Table 1. Luminescence decay times (at room temperature) for several storage phosphor materials^{4, 5, 6} ($\text{BaFBr}_{1-x}\text{Eu}^{2+}$ is the most commonly used in today's CR systems)

As illustrated above, the image quality of a CR system is a complex combination of, and often a trade-off between, material properties, hardware design, and processing software. Nevertheless, the image quality of CR systems has improved considerably over the last twenty years. Advances in storage phosphor chemistry, screen design, and manufacturing techniques have contributed especially to this improvement. If we use the increasingly accepted criterion of Detective Quantum Efficiency⁸ (DQE) as a measure of image quality, then this improvement can be made more quantitative.

The DQE results reported for first-generation, flying-spot CR systems⁹ were modest compared to existing screen/film systems. The DQE value at an exposure of 1 mR (10 μ Gy) and a spatial frequency of 0 cy/mm, DQE(0), was about 11%. At 2 cy/mm, that value went down to around 5%. This tended to limit the clinical uses of these initial CR systems to applications that benefited from CR's wide exposure latitude, but that were less dose- and resolution-sensitive (e.g., portable radiography). An interesting study¹⁰ of four more recent generations of CR systems (scanners and IPs) reported that the cumulative, relatively small improvements in scanner hardware and IPs had increased DQE(0) values by approximately 30%, while DQE values at higher frequencies had almost tripled. Thus, CR systems had become clinically competitive with screen/film systems for many more diagnostic applications, even as screen/film systems had improved their DQE performance over time. Current DQE(0) values for state-of-the-art flying-spot CR systems are in the range of 25-28%. A more recent study¹¹ claims DQE(0) values that are 30-40% higher than current values through the use of a transparent support material for the IP. By reading the phosphor layer from both sides simultaneously (i.e., dual collection optics and dual photodetectors), both the signal and SNR are improved (the MTF does not change significantly, since the light scattering in the screen remains and the signal transmitted through the screen has little high-frequency content).

2. THE NEW SCANNING ENGINE

A number of the above limitations shared by flying-spot scanners can be overcome by using a novel scanning technique in which the IP is scanned **one line at a time**, rather than one point at a time. In particular, the size limitations imposed by the bulkier flying-spot components are no longer relevant. Furthermore, the trade-offs between throughput and image quality can be largely circumvented. For example, dwell times in the new technique are measured in milliseconds rather than microseconds, yet scan times are still significantly shorter than those of flying-spot scanners. In fact, with the new needle-based CsBr:Eu²⁺ storage phosphors, the new scan engine produces image quality (DQE) that is comparable to that of the latest flat-panel DR systems based on CsI:Tl and amorphous Si flat-panel arrays^{3, 12}.

Figure 4 shows a diagram of the concept and Figure 5 shows an actual prototype of the new scanning engine, dubbed ScanHead[®]. The laser sources, beam-shaping optics, intensity control, light collector, filter, and photodetectors are all contained in one compact unit that scans quickly (43 x43 cm in approx. 5s) over a stationary IP. The control electronics to pre-process the captured signal are also on board, so that the raw, 14-bit digital image data can be transferred directly from the ScanHead[®] to a control computer for further processing and distribution. In the following sections, we will describe some of the important design considerations for several of the major components of this new scan engine.

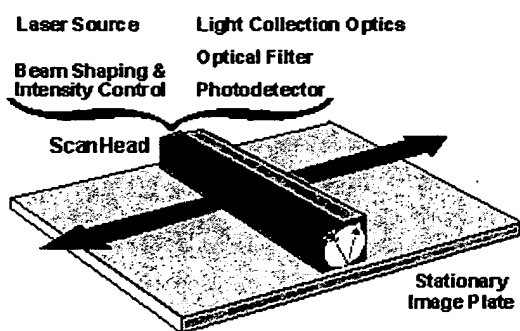


Figure 4. Schematic diagram of the new scanning concept. The compact, movable ScanHead[®] module contains lasers, beam shaping optics, intensity controllers, a light collector, an optical filter, and a photodetector.



Figure 5. Laboratory prototype of the ScanHead[®] module.

2.1 Laser source, beam shaping, and intensity control

The light source is used to stimulate the storage phosphor locally to emit its stored energy. Although much of the installed base of CR systems still uses gas lasers for this task, newer CR systems are all based on laser diodes. These are available at wavelengths (red) and output powers (tens of mW) that are well matched to the stimulation spectra and sensitivities of today's storage phosphor materials. In addition, they are very compact light sources.

For ScanHead[®], where an entire line must be illuminated at once, a linear array of laser diodes is used (Fig. 6). Although the sampling resolution of the CCD (Charge-Coupled Device) photodetector is 50 μm (see Sect. 2.4), providing one laser diode for each detector element would be cost-prohibitive and unreliable. Instead, we use the divergent, strongly asymmetric output beam profile of laser diodes to reduce the number of emitters to several dozen. The diodes are placed so that the strongly diverging (horizontal) beams overlap along the ScanHead[®] axis, producing a continuous line of stimulating light with sufficient power to reach an acceptable read-out depth in the IP. By inserting two plano-convex cylindrical lenses into the beam path, it is possible to focus the less diverging (vertical) beam axis down to 80 μm transverse to the line to maintain a reasonable MTF in that direction (as already indicated, the actual line width within the screen is largely determined by light scattering).

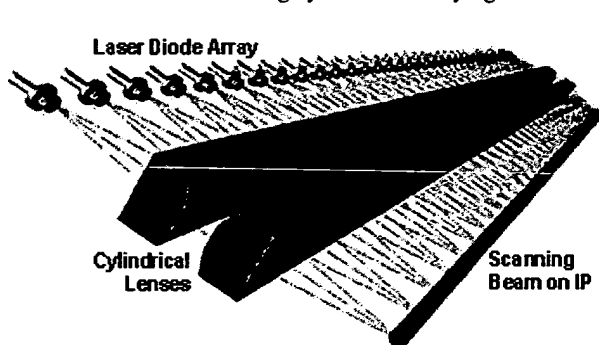


Figure 6. Schematic diagram of the linear laser diode array and the optics used to stimulate each line on the image plate. The large beam divergence along the lens axis creates the continuous scanning line. The smaller beam divergence across the lens (the rays in the figure) is brought to focus at the IP surface.

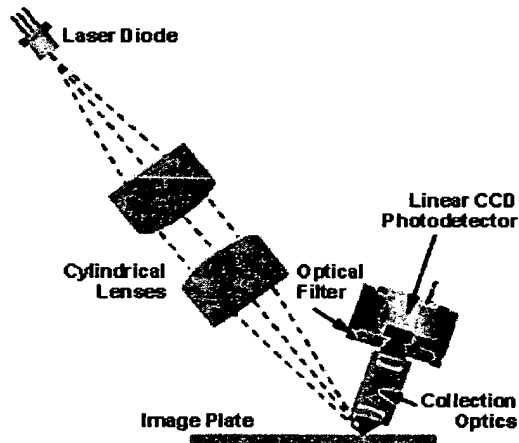


Figure 7. Cross-section of ScanHead[®] showing the angulation of the stimulation and detection sections.

Intensity control is needed to minimize static and dynamic exposure fluctuations to the IP. Such fluctuations easily can cause visible banding artifacts in the image. Static intensity variations along the scan line can occur, for example, from variability in the laser diode outputs and from overlap of the beam profiles of neighboring diodes. As in flying-spot scanners, such static intensity variations can be calibrated out by measuring the scanned line profile for a flat-field exposure and correcting all subsequent scanned data according to the measured profile. The tolerance for variability is fairly large here, on the order of 10-15%. The tolerance for dynamic fluctuations is considerably tighter. With an operating point on the linear part of the stimulability curve (Fig. 2), the allowable intensity variations may be less than fractions of 1%. ScanHead[®] operates near the saturated part of the stimulability curve (high read-out depth), which lowers this tolerance to around 1%. Correction of such dynamic intensity fluctuations must be done using active feedback, which can be done fairly straightforwardly in laser diodes, since they are driven directly.

Because of the compact nature of the ScanHead[®] module, it is difficult to achieve the usual beam geometry of a flying-spot scanner (stimulating beam nearly perpendicular to the IP). For the reflective configuration we have assumed so far, the stimulation and detection sections in ScanHead[®] are on the same side of the IP and must, therefore, be angled relative to the plate normal. This can be inferred from the photograph in Fig. 5 and seen more clearly in Fig. 7, which illustrates a view along the ScanHead[®] axis. Suitable angles for the stimulation and collection sections were determined by balancing the optical behavior of the incident beam (flare, scatter), the signal output at the photodetector, and MTF.

2.2 Light-collection optics

Once stimulated, the IP emits (blue) light in proportion to the stored x-ray exposure. This light emission is roughly Lambertian, that is, it is emitted in all directions. The purpose of the light-collection optics is to collect and direct as much of this emitted light as possible onto the active surface of the photodetector. In flying-spot scanners, this is usually done with acrylic light pipes, fiber optics, mirrors or integrating cavities. As in a flying-spot scanner, maximum light collection efficiency is realized when the entrance surface of the collection optics is as close to the IP surface as possible (i.e., the numerical aperture is large). For the same reason, the exit surface must be (at least, optically) close to the photodetector. The size constraints of ScanHead[®] add additional complexity, as already indicated. This produces a configuration for the reflective scanning geometry as shown in Fig. 7.

One solution for light collection involves an array of tiny gradient-index (GRIN) lenses, e.g., SELFOC[®] microlenses¹³, positioned along the illuminated line. These tiny (~1 mm diameter) lenses act like focused fiber optics that collect the light emitted from the scan line and image it, at unit magnification, onto the individual elements of the photodetector. In order to capture enough of the light emitted from the stimulated line, this SELFOC[®] array must contain multiple rows of hexagonally close-packed GRIN lenses across the entire 43 cm width of the scan line. In this configuration, the collection efficiency of the SELFOC[®] array is about 10%. This relatively low value is partly due to the empty interspaces between the lenses. In addition, GRIN optics are fairly dispersive for the main wavelengths (~ 400-450 nm) emitted by the storage phosphors of interest.

Another solution is the use of linear microlens arrays. The light transmission characteristics of such arrays can be significantly better (~2x) than GRIN optics, albeit at significantly higher cost. This is the solution chosen for ScanHead[®]. Fig.8 shows a small section of one possible microlens configuration for the "Collection Optics" block from Fig. 7. The array of microlenses is clearly visible between the two axial cylindrical lenses. The light collection efficiency in the direction perpendicular to the scan line is determined essentially by the height of the axial cylindrical lenses. Along the scan line, the efficiency is determined primarily by the width of each microlens. With appropriate angulation and spacing of the collection optics relative to the IP, the collection efficiency of the microlens array in ScanHead[®] is greater than 20%, comparable to that of light collection systems in flying-spot scanners.

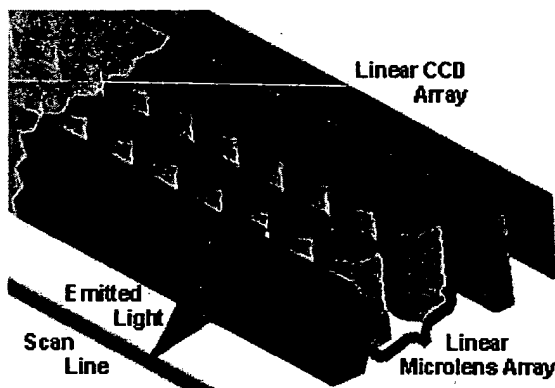


Figure 8. Linear microlens array used in the collection optics of ScanHead[®]. Behind the collection optics (optical filter not shown) is the CCD photodetector.

2.3 Optical Filter

The purpose of the optical filter is to block all light that is not stimulated emission from the IP. This is critical since the ratio between the stimulating (red) light intensity and the emitted (blue) light intensity is greater than 10^8 . This means that the optical filter must have high transmission for the emitted wavelengths (400-450 nm, depending on the storage phosphor) and extremely low transmission for all other wavelengths to which the photodetector is sensitive.

The design of the optical filters for ScanHead[®] is more difficult than for all current flying-spot scanners. For one, current flying-spot scanners are designed to scan only one storage phosphor material (either BaFBrI:Eu²⁺ or RbBr:Ti). ScanHead[®], on the other hand, will be configurable for two storage phosphor materials, BaFBrI:Eu²⁺ and the new CsBr:Eu²⁺ needle-based phosphors, that have different emission characteristics³. Secondly, IR radiation plays a more significant role in ScanHead[®] (for example, the laser diode stimulation source produces IR radiation in addition to the visible). IR radiation is not a problem in laser-diode-based flying-spot scanners using photomultiplier tubes (PMTs) as photodetectors, since their response decreases rapidly above 650 nm. However, the CCD photodetectors used in ScanHead[®] are still quite sensitive in the IR, so the filter solution must block these wavelengths in addition to the stimulating light.

2.4 Photodetector and on-board electronics

The photodetector in ScanHead[®] (see Figs. 7 and 8) is an array of six custom-designed, low-noise, linear CCD sensors with on-board processing electronics and built-in temperature sensors. The six CCDs are butted end-to-end in a special housing to provide a practically continuous line of detector elements along the illuminated scan line (dead zones no larger than 70 μ m). Each CCD contains 1464 asymmetric, active photo-elements measuring 50 μ m x 400 μ m, with the small dimension oriented along the illuminated scan line (the "fast-scan" direction in a flying-spot scanner). The asymmetry of the active elements allows the system to maintain high resolution along the scan line while still collecting enough emitted light per pixel to keep the system gain and SNR at reasonable levels (the resolution in the slow-scan direction is determined to first order by the width of the illuminated line and by light scattering within the phosphor layer). The signals from the 8784 individual elements (pixels) along the line can be combined in several different ways, leading to in-line sampling resolutions of 50, 100 or 150 μ m per pixel.

With appropriate driving circuitry and operating points, the dynamic range of the ScanHead[®] CCDs is over 10⁴, comparable to the PMTs used in flying-spot scanners, and well matched to the dynamic range of the storage phosphor screens used in diagnostic imaging. Thus, no special pre-scanning or gain setting is required to determine the actual exposure range on an IP. The quantum efficiency of the photodetectors for the emission wavelengths of interest is greater than 60%, which is better than that of PMTs in the same wavelength range.

The on-board electronics in ScanHead[®] take the analog video signal emerging from the CCDs, sample it and quantize it to 14 bits. Special effort was made in the board designs to keep electronic noise to a minimum. For example, since the internal noise of CCDs is normally greater than that of PMTs, the A/D converter uses correlated double sampling¹⁴ to improve the read-out SNR. In this scheme, both the total signal value and the dark current (offset) are measured for each pixel, and then subtracted to produce the signal value that is quantized.

2.5 Other Scanner Components

While the ScanHead[®] is novel and interesting technology in and of itself, it is useless without the appropriate hardware and software that enable construction of a complete CR system. For example, the ScanHead[®] module must be moved at constant velocity along the IP (slow-scan transport). It must also maintain a constant height above the IP. Even small fluctuations in velocity or height can lead to visible banding in the image. The IP must be positioned and affixed to the scanning stage during ScanHead[®]'s movement. Furthermore, the scanned IP must be erased before re-use. This requires a new, integrated erase unit in a size consistent with ScanHead[®]'s (erase modules in current flying-spot systems are too large for ScanHead[®]-based systems). Solutions for some of these issues will be covered in more detail in forthcoming publications.

3. IMAGE QUALITY EVALUATION

One important measure of the imaging performance of a new capture system is its objective image quality relative to other systems designed for the same purpose. A suitable metric for such comparisons is Detective Quantum Efficiency. Here we must distinguish between the DQE results achieved with conventional powder IPs, where the phosphor layer consists of small phosphor particles embedded in a binder, and those achieved with needle IPs, where the phosphor layer is grown in tiny, vertical needles on a substrate, without the need for a binding material. The image quality results for the two are quite different³.

Shown in Fig. 9a are the DQE results for three different CR systems: a state-of-the-art flying-spot scanner reading a BaFBr_xI_{1-x}:Eu²⁺ powder IP (Agfa ADC Compact/MD-30 screen), a prototype ScanHead[®]-based reader scanning the same (MD-30) powder IP, and the same reader scanning a prototype CsBr:Eu²⁺ needle IP. All data were acquired at 70 kV_p with a 0.5 mm Cu filter at a dose of 1 μ Gy. The Scan Head[®] collection optics for both screens were fitted with an early prototype linear microlens array and, to illustrate the impact of this component on image quality, both the in-line ("fast-scan") and slow-scan DQE results are shown for the ScanHead[®]/Needle IP configuration (see below). The experimental procedures used to measure the MTF and NPS, and the methodology to calculate DQE in the CR systems have been described in more detail elsewhere³.

As can be seen in the figure, the combination of ScanHead[®] (with a microlens) and a powder IP produces DQE results that are comparable to, or somewhat better than today's flying-spot systems scanning powder IPs. The DQE results for

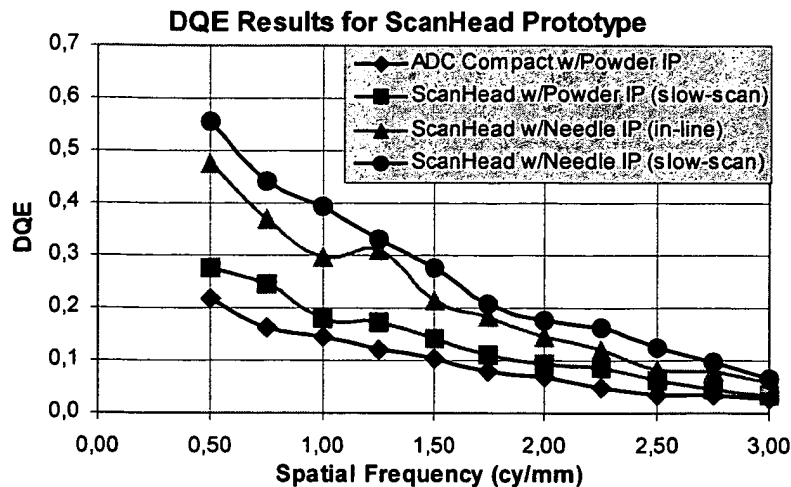


Figure 9a. DQE results for three imaging systems: CR using a flying-spot scanner (ADC Compact) and a conventional (MD-30) powder IP, CR using a ScanHead[®] prototype and a conventional (MD-30) powder IP (only slow-scan DQE shown), CR using a ScanHead[®] prototype with a prototype CsBr:Eu²⁺ needle IP (in-line and slow-scan DQEs are shown). The difference between in-line and slow-scan DQE for this ScanHead[®] system is due to the linear microlens used for these measurements (see text). All data were acquired at a dose of 1 μ Gy at 70 kV_p with a 0.5 mm Cu filter.

ScanHead[®] and Needle IP are significantly better (2-3x) than those produced with powder IPs. This improvement is due largely to the superior imaging properties of the new needle screens³ but also to the imaging performance of ScanHead[®]. Note that the slow-scan and in-line DQE for this ScanHead[®] module are different. The linear microlens array used in this prototype scanner had suboptimum MTF characteristics along the in-line direction, causing a decrease in DQE. More recent versions of this array have shown better optical properties, and we expect the in-line results in future ScanHead[®] units to be equivalent to those in the slow-scan direction.

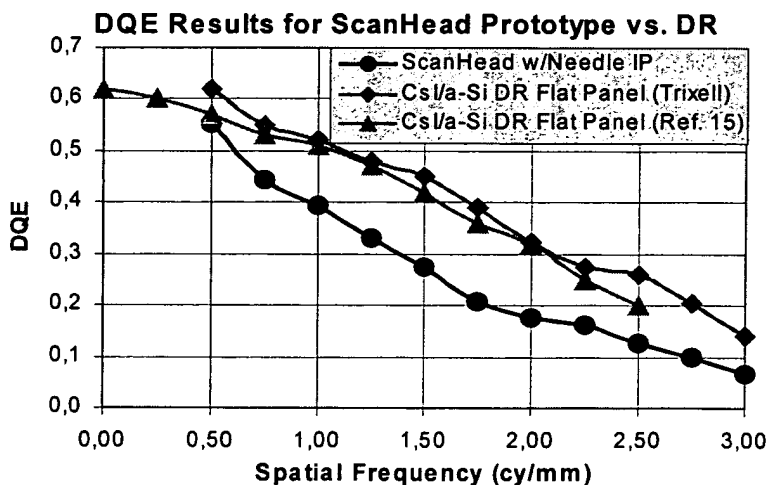


Figure 9b. DQE results (at 1 μ Gy) for a ScanHead[®] prototype with a prototype needle IP, along with two flat-panel DR systems based on CsI and an amorphous Si photodetector/converter¹⁵. The DQE data for the Triexell detector (\blacklozenge) were acquired in-house using the same methodology as in the CR measurements shown in Fig. 9a.

It is also interesting to compare the ScanHead[®]/Needle IP DQE results with those of DR systems. Unfortunately, DQE comparisons between systems can be difficult and dangerous to interpret due to differences in exposure, measurement and data analysis techniques. With this caveat, Fig. 9b shows a comparison of the ScanHead[®]/Needle IP results from Fig. 9a (slow-scan) and literature values¹⁵ on one flat-panel DR system based on a CsI:Tl x-ray detector and an amorphous Si photodetector array. Another DR flat panel (from Trixell) was measured on an in-house system with the same methodology used for the three CR systems shown in Fig. 9a. These results are also shown.

Although there is currently a gap (30-50%) between the ScanHead[®] and DR DQE curves in Fig. 9b, particularly at mid-frequencies, it is important to note that the CR data were created on a laboratory version of the device using early prototype needle screens. We expect the ScanHead[®] DQE values to increase as the needle IPs improve (increase in gain and sharpness) and as the optical filters improve (decrease in electronic noise). Despite the current gap, the visual image quality of the ScanHead[®]/Needle images is comparable to that of DR systems. A recent contrast-detail study comparing a conventional flying-spot scanner using powder IPs, a ScanHead[®] scanner using Needle IPs, and several flat-panel DR systems suggests that this objective image quality parity carries over into observer performance for detection tasks with low-contrast targets in noisy backgrounds¹².

4. APPLICATIONS AND DEVICES

A compact scanning technology like ScanHead[®], with its high level of image quality, can be used in practically any diagnostic imaging application and in multiple device configurations. The simplest configuration is a single-slot, cassette-based scanner for distributed or low-volume imaging applications (e.g., in the exam room). One possible design for such a scanner is illustrated in Fig. 10. Note that the scanning engine (ScanHead[®]), its slow-scan transport system, an erase unit, the IP handling/positioning unit and platform, and all associated electromechanical and electronic systems fit inside a floor-standing scanner "tower." The scanner can be adapted to read conventional powder IPs or needle IPs, assuming the same cassette design. With appropriate cassette buffering, centralized, high-volume configurations can also be realized with the same basic components.

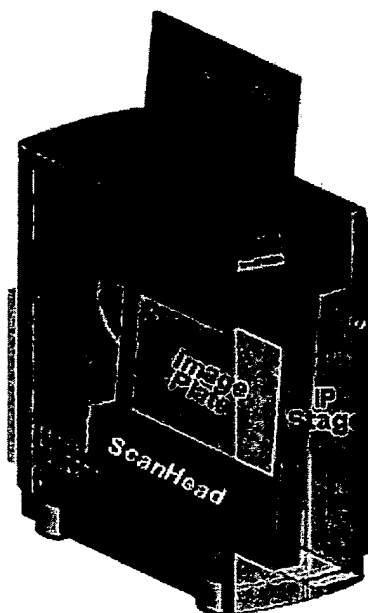


Figure 10. A view through the semi-transparent case of a single-slot CR tower reader based on ScanHead[®] technology. The tower contains the scanning engine, the scanning stage, slow-scan transport hardware, an erase unit, IP handling and positioning subsystems, and all associated electronics.

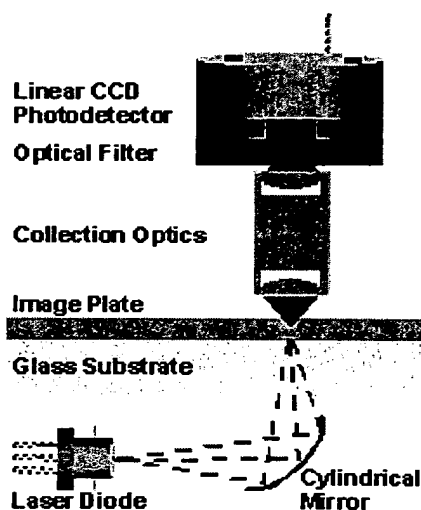


Figure 11. Possible transmission-mode scanning geometry using a cylindrical mirror. The stimulation section of ScanHead[®] is below, the collection section above the IP.

ScanHead[®] technology also enables some devices that were previously impossible with flying-spot CR technologies. For example, flat-panel, cassetteless CR systems can now be realized. For these devices, a transmissive ScanHead[®] configuration is more useful than the reflective one discussed so far. In this configuration, the stimulation and collection sections are on opposite sides of the IP. Fig. 11 shows a possible beam geometry of such a system and Fig. 12 shows a prototype of a ScanHead[®]-based flat-panel CR system that might be used for portable radiography or as the capture

module inside a Bucky table. For flat-panel systems, the IP must be optically accessible from both sides, so the substrate must be transparent, e.g., glass. Since the needle-based storage phosphor, CsBr:Eu²⁺ can be deposited very effectively on glass substrates, and produces excellent image quality, it is the ideal candidate for the CR flat-panel. The radiation sensitivity of the CCDs can be dealt with by parking the ScanHead[®] module in a shielded area during the x-ray exposure. One can also imagine other possible ScanHead[®] device configurations suitable for a dedicated chest unit, mammography systems, etc.

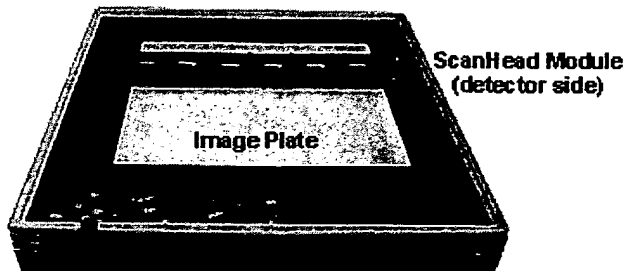


Figure 12. View inside a CR flat panel containing the ScanHead[®] module. The stimulation section is underneath the image plate.

5. CONCLUSIONS

We have described a new type of CR scanning engine using a **line-at-a-time** scanning principle, instead of the point-at-a-time technique used by all current CR systems. This produces a number of significant advantages over current flying-spot scanners. The size of scanners using this ScanHead[®] technology can be considerably smaller than current systems due to the fact that the stimulation and collection subsystems are contained in one compact module. Despite the size reduction, scanner throughput can still be quite high since many pixels are captured simultaneously.

The image quality of a ScanHead[®] system can be equivalent to current CR systems when using conventional powder IPs, and can be significantly better than current CR systems when using needle IPs. The high level of image quality achieved with needle IPs is largely due to the properties of the needle IP itself, but also due to the imaging characteristics of ScanHead[®] (longer pixel integration time, higher read-out depth, good MTF, low-noise electronics). With appropriate collection optics, the image quality with needle IPs can be comparable to that of recently introduced flat-panel DR systems based on CsI:Tl and amorphous Si photodetectors. While image quality is certainly not the only criterion for the clinical applicability or acceptability of a new technology, it is not an insignificant one. The variety of device configurations possible with ScanHead[®] technology, from centralized, high-volume systems to distributed, single-plate readers to cassette-less flat panels, and its significantly lower cost compared to current DR systems, suggest that future CR systems will continue to play an important role in the acquisition of diagnostic images.

ACKNOWLEDGEMENTS

We wish to thank Magath Niang for performing the DQE measurements. We also wish to thank Dr. Georg Reiser for helpful conversations on ScanHead[®] optics. Thanks also to Christian Bommer for help with the 3-d microlens graphic.

REFERENCES

1. R. Schaetzing, B. R. Whiting, A. R. Lubinsky, J. F. Owen, "Digital Radiography Using Storage Phosphors," *Digital Imaging in Diagnostic Radiology*, eds. J. D. Newell, C. A. Kelsey, pp. 107-138, Churchill Livingstone, New York, 1990.
2. M. Sonoda, M. Takano, J. Miyahara, H. Kato, "Computed Radiography Utilizing Scanning Laser Stimulated Luminescence," *Radiology* **148**:3, pp. 833-838, 1983.
3. P. Leblans, L. Struye, "New Needle-crystalline CR Detector," *Proc. SPIE* **4320**, pp. 59-67, 2001.
4. H. von Seggern, T. Voigt, K. Schwarzmichel, "Physical Mechanisms of Photostimulation in Medical X-Ray Storage Phosphors," *Siemens Forsch.-u. Entwickl.-Ber.* **Bd 17**:3, p.125, 1988.

5. H. von Seggern, "Photostimulierbare Speicherleuchtstoffe für Röntgenstrahlung," *Phys. Bl.* **48:9**, pp. 719-723, 1992.
6. P. Leblans, private communication.
7. M. I Sezan, A. M. Tekalp, "Survey of Recent Developments in Digital Image Restoration," *Opt. Eng.* **29(5)**, pp. 393-404, 1990.
8. J. C. Dainty, R. Shaw, *Image Science*, Academic Press, London, 1976.
9. H. Kato, "Photostimulable Phosphor Radiography Design Considerations," *Proc. AAPM Summer School*, pp. 860-898, 1991.
10. J. T. Dobbins III, D. L. Ergun, L. Rutz, D. A. Hinshaw, H. Blume, D. C. Clark, "DQE(f) of Four Generations of Computed Radiography Acquisition Devices," *Med. Phys.* **22(10)**, pp. 1581-1593, 1995.
11. S. Arakawa, W. Itoh, K. Kohda, T. Suzuki, "Novel Computed Radiography System with Improved Image Quality by Detection of Emissions from Both Sides of an Imaging Plate," *Proc. SPIE* **3659**, pp. 572-581, 1999.
12. R. Schaetzing, R. Brandl, K.-J. Pfeifer, P. Leblans, "Improving the DQE and Low-Contrast Detectability of CR Systems Through the Use of Structured (Needle) Storage-Phosphor Screens," *Radiology* **221(P)**, 463, 2001.
13. *SELFOC* is a registered trademark of Nippon Sheet Glass Co., Ltd., Japan.
14. Specifications Datasheet for Analog Devices AD9814 CCD/CIS Signal Processor, Rev. 0, Analog Devices Inc., Norwood, MA, 1999.
15. K. S. Kump, "Fast Imaging of a 41cm Amorphous Silicon Flat-Panel Detector for Radiographic Applications," *Proc. SPIE* **4320**, pp. 87-93, 2001.

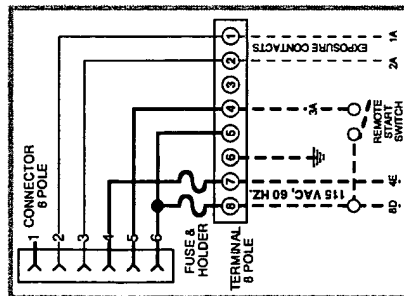
POERSCH RECIPROCATING BUCKYS, MODELS RRJ & RRK SERVICING AND REPLACEMENT PARTS

115 VOLTS A.C.

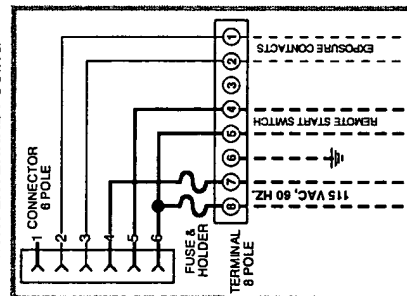
TERMINAL MODULE
P/N 8284R19



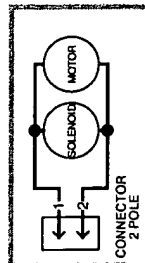
REPLACEMENT FUSES
THERMAL OVERCURRENT
5 x 20 mm 500 mA 250 Volts
P/N 8284R19-01



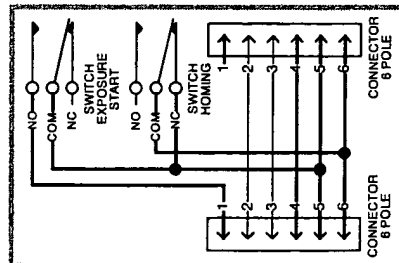
ALTERNATE 5 WIRE HOOK-UP
WITH EXTERNAL FUSING



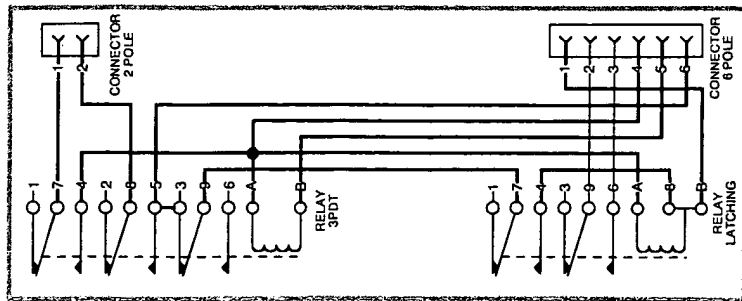
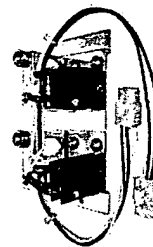
6 WIRE HOOK-UP



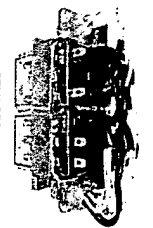
DRIVE MODULE
P/N 8284R48



SWITCH MODULE
P/N 8284R39

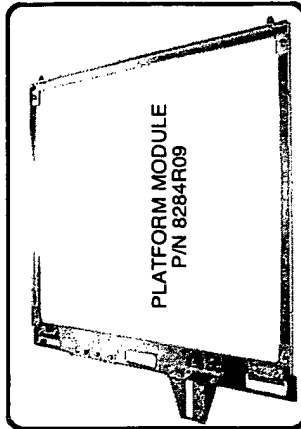


RELAY MODULE
P/N 8284R29

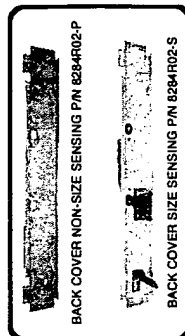


SCHEMATIC WIRING DIAGRAM

- LEGEND
- 115 VAC Wiring, By Manufacturer
 - 115 VAC Wiring, By Others
 - Low-Voltage Wiring, By Manufacturer
 - Low-Voltage Wiring, By Others



PLATFORM MODULE
P/N 8284R09

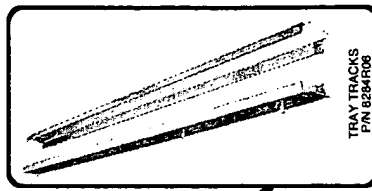


BACK COVER NON-SIZE SENSING P/N 8284R02-P

BACK COVER SIZE SENSING P/N 8284R02-S



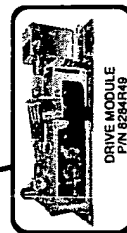
ION CHAMBER
CHANNELS
P/N 8284R05



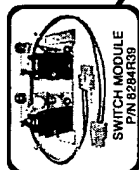
TRAY TRACKS
P/N 8284R06



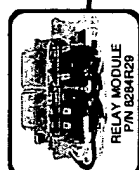
TRAY STOP
P/N 8284R04



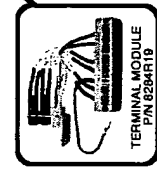
DRIVE MODULE
P/N 8284R48



SWITCH MODULE
P/N 8284R39



RELAY MODULE
P/N 8284R29



UNDER PLASTIC SHIELD



TERMINAL MODULE
P/N 8284R19

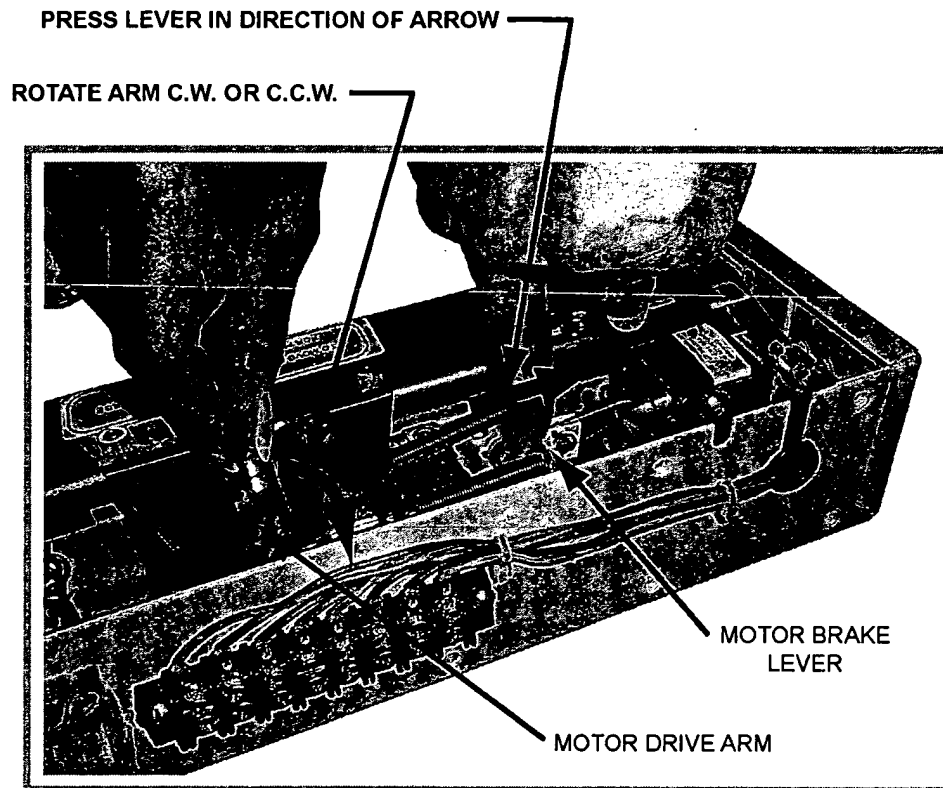
When ordering replacement parts provide MODEL AND SERIAL NUMBER
For service and parts contact:

Poersch Metal Mfg. Co.
4027 W. Kinzie St.
Chicago, IL 60624 USA
Phone: 773.722.0890, Fax: 773.722.4122
Web: www.poerschmetal.com

BEST AVAILABLE COPY

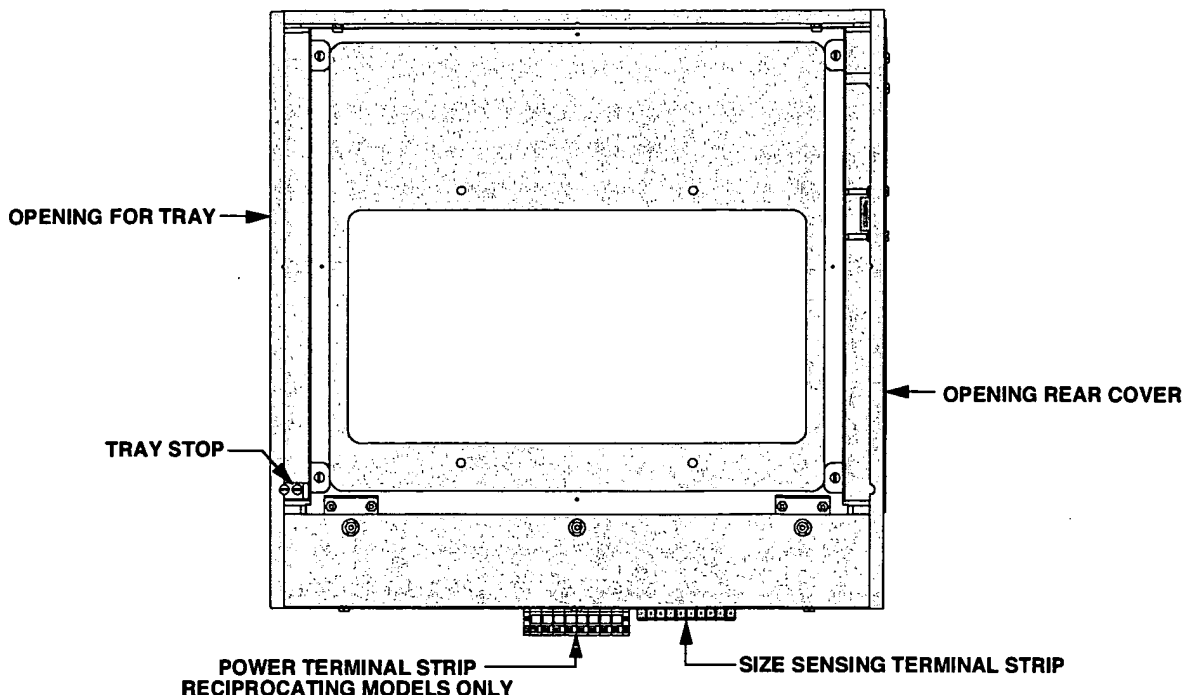
INSTRUCTIONS

HOW TO MANUALLY MOVE RECIPROCATING PLATFORM



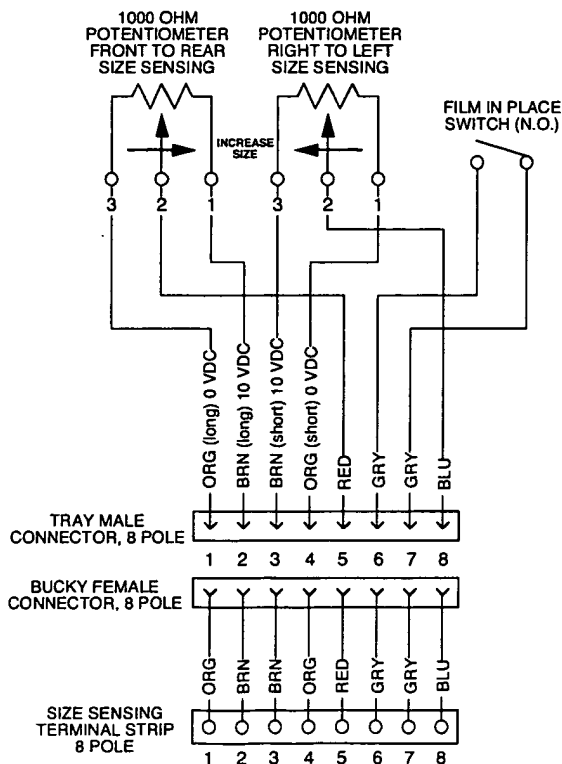
- STEP 1** DISCONNECT POWER TO BUCKY.
- STEP 2** Remove bucky motor compartment top cover.
- STEP 3** Release motor brake by pressing lever back with finger, in direction of arrow, away from springs. (see photo above)
- STEP 4** Rotate motor drive arm in either direction. (see photo above)
Note, bucky will automatically reset itself when power is turn on.

BEST AVAILABLE COPY



BUCKY - LEFT HAND LOADING

TURN PAGE FOR INSTRUCTIONS
HOW TO SWITCH LOADING SIDE FROM LEFT TO RIGHT

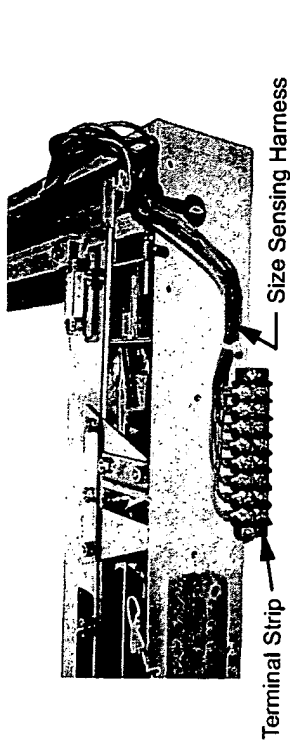


OUTPUT VOLTAGE

With 10 ± 0.01 VDC applied across potentiometers (pins 1 and 2 for front to rear sizing; pins 3 and 4 for right to left sizing), the voltage measured between terminals 1 and 5 (for front to rear sizing) and 4 and 8 (for right to left sizing) for various cassette sizes listed below.

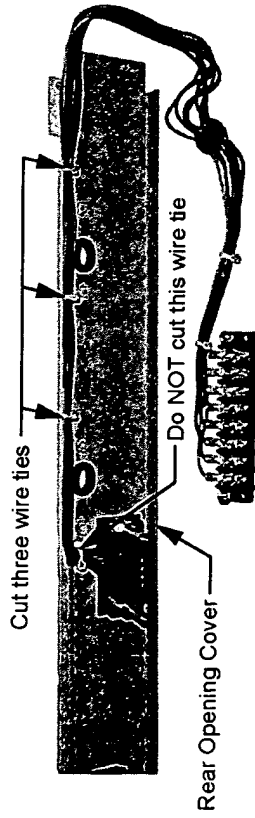
CASSETTE SIZE (OUTSIDE DIM.)	STATED FILM SIZE	OUTPUT VOLTAGE ± 0.2	OHMS VALUES
154.5 mm	5 in.	0.60	940
157.5 mm	13 cm	0.69	931
205.3 mm	7 in.	2.06	794
207.5 mm	18 cm	2.12	788
230.7 mm	8 in.	2.80	720
268.8 mm	24 cm	3.90	610
281.5 mm	10 in.	4.26	574
306.9 mm	11 in.	5.00	500
327.5 mm	30 cm	5.60	440
332.3 mm	12 in.	5.70	430
383.1 mm	35 cm	7.02	298
459.3 mm	43 cm	9.40	60

WIRING SCHEMATIC FOR SIZE SENSING MODEL RRJ BUCKYS, MODEL RSJ GRID CABINETS AND MODEL QJ TRAYS



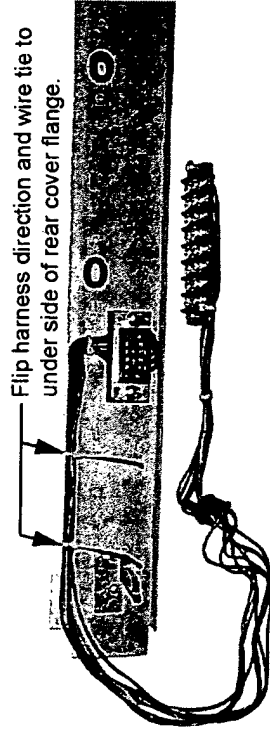
STEP 1

Remove bucky motor compartment top cover and unscrew size sensing terminal strip from outside of bucky (Note: do NOT disconnect wires from terminal strip). Cut two wire ties binding size sensing harness inside motor compartment. Remove grommet and lift out harness from hole on side of bucky.



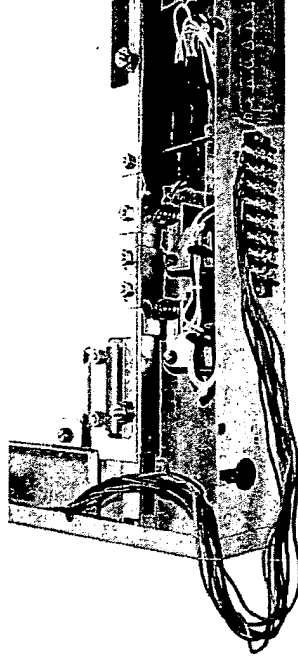
STEP 2

Unscrew four screws fastening tray opening, rear cover to bucky, remove rear cover from bucky. Cut three wire ties binding harness along top flange of rear cover. Do NOT cut wire tie above the blue female connector assembly.



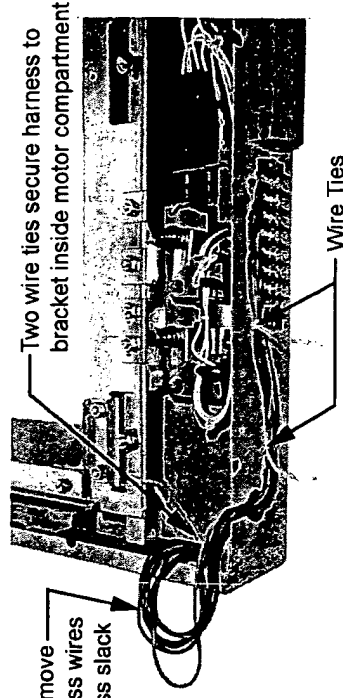
STEP 3

Flip size sensing harness 180° to other direction and wire tie securely along under side of rear cover top flange.



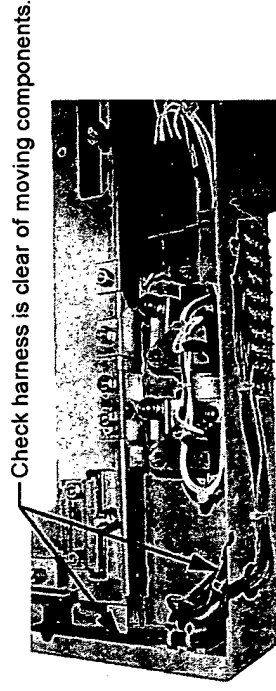
STEP 4

Unscrew "tray stop" from bottom of tray side of bucky, refasten stop at opposite diagonal corner. Reinstall rear cover into opposite opening of bucky and fasten size sensing terminal strip to outside of bucky.



STEP 5

Remove grommet and dress harness wires thru hole on side of bucky, reinsert grommet. Secure harness with two wire ties inside motor compartment and two wire ties outside bucky. BEFORE pulling wire ties tight remove slack from each wire of harness as shown above.



STEP 6

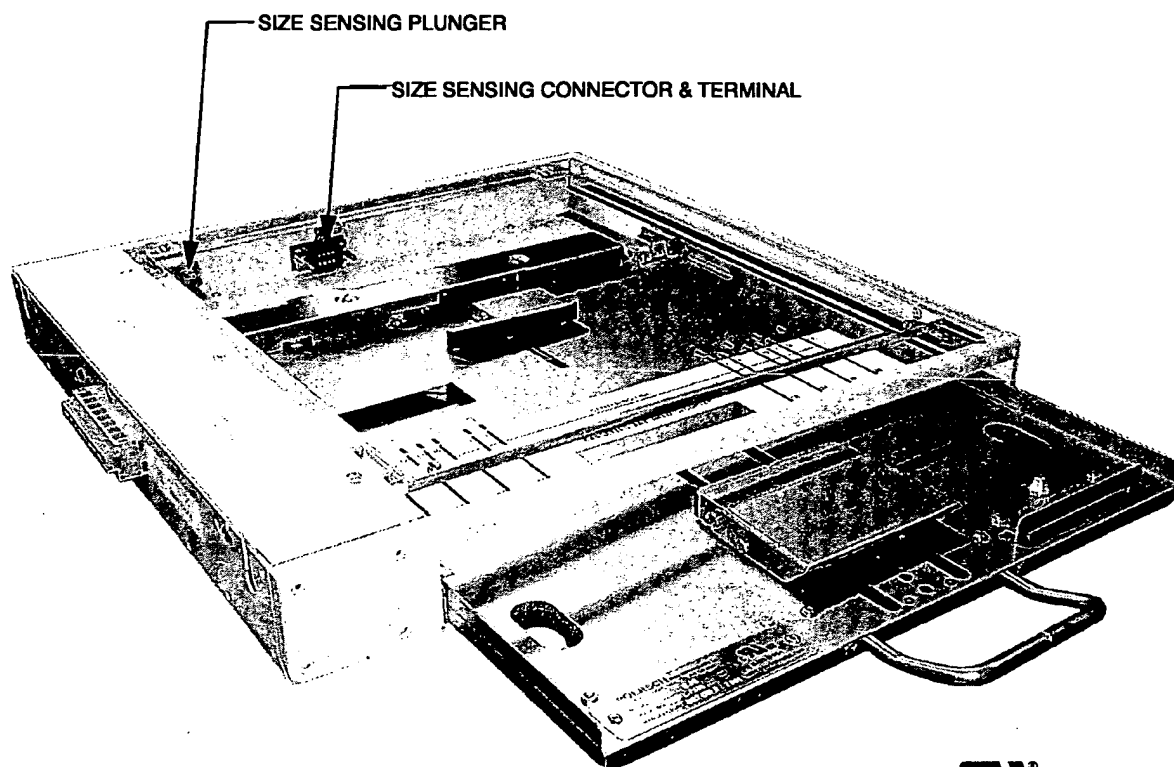
Tightly bundle harness excess wire and secure inside motor compartment away from all moving components. Replace and fasten top cover securely.

INSTRUCTIONS

HOW TO SWITCH BUCKY LOADING SIDE FROM LEFT TO RIGHT

FOLLOW SIMILAR PROCEDURE WHEN SWITCHING FROM RIGHT TO LEFT

POERSCH Metal Manufacturing Co.
 4027 WEST KINZIE STREET, CHICAGO, IL 60624, USA
 PHONE: 773.722.0890; FAX: 773.722.4122
 www.poerschmetal.com



RECIPROCATING BUCKY MODEL RRJ

Shown with automatic size sensing cassette tray partially inserted
 (cassette tray not included)

DESCRIPTION	PART NO.
AUTOMATIC SIZE SENSING INSTALLATIONS	RRJ
MANUAL SIZE SENSING INSTALLATIONS	RRK

The Poersch reciprocating bucky is designed for use in Radiographic Tables and Vertical Bucky Stands. Available in two models; model RRJ is compatible with automatic size sensing cassette trays and model RRK is compatible with manual non-size sensing cassette trays. Both models are identical in construction and size. The plunger, connector and terminal required for automatic size sensing are not included on the model RRK.

The cassette loading, is easily switched from right hand to left hand by transferring the rear cover and tray stop to opposite ends. Under normal conditions no maintenance is required. All drive components are rated for continuous duty and life tested for greater than one million exposures.

BEST AVAILABLE COPY

[illegible]

BEST AVAILABLE COPY